FSI-based Overflow Assessment of the Seismically-Isolated SFP with Fuel Racks

Gil Y. Chung [a*], Hyun T. Park [a], Soo-Hyuk Chang [a], Sang-Hoon Lee [b]

[a]Korea Maintenance Co., Ltd., Engineering Design Dept., 263 Gamasanro, Guro-Gu, Seoul, Korea, 152-842
[b]KEPCO E&C, Civil/Arch. Eng. Dept.,8 Kumiro, Bundang-Gu, Sungnam, Gyeonggi-Do, Korea, 463-870
[*]Corresponding author: cgy@kmctech.co.kr

1. Introduction

To date, effectiveness of the seismic isolation systems for reducing seismic force effectively has been well demonstrated. In this context, practical application of the technology in nuclear engineering fields has become an important issue more and more. Obviously, lifetime structural performance in nuclear isolation systems will be improved. However, assuming that a nuclear liquid storage tank, spent fuel pool (SFP), containing radioactive material is seismically isolated, overflow-induced damages under earthquake may happen inevitably. This is because fluid motion can be rather amplified due to the increased relative displacement between the base and superstructures by a long-period shift. Therefore, overflow assessment and prediction of the seismically-isolated SFP have to be conducted in design phase.

For performing sloshing-induced overflow of the seismically-isolated SFP, a fluid-structure interaction (FSI) approach making a two-way coupling process between structural and fluid solvers is herein employed. In this study, fuel racks inside the SFP are included in FSI modeling to investigate effect of fuel-cell assemblies on SFP overflow. Accordingly, three different assembly sets of fuel cells are assumed to be inserted in fuel racks. In addition, floor acceleration time-histories produced from three different amplitudes of peak ground acceleration (PGA) are applied to the SFP base to investigate load effect on liquid overflow.

2. Methods and Results

The seismically-isolated SFP with fuel racks can experience sloshing-induced overflow in potential seismic risk regions. Based on FSI approach, effects of fuel racks and PGAs on its overflow damage are herein investigated.

2.1 FSI Approach for Overflow Assessment

For the seismically-isolated SFP, sloshing-induced overflow can be well quantified by performing FSI analysis which solves a multi-physics problem associated with the interaction between deformable structures and fluid flow [1]. The computational fluid dynamics (CFD) approach is also used to consider multiphase flow phenomena of gas/air and liquid [2]. In this study, FSI analysis is conducted by coupling two analytical solvers, as shown in Fig. 1 [2,3]. In structural analysis, all necessary boundary and loading conditions are imposed at the base of a tank, while volume of fluid (VOF) method in sloshing analysis is employed due to its suitability for determining the shape and location of free surface [4]. In the FSI coupling process, individual outputs including mesh displacement and force are continuously transferred to the structural and fluid solvers, respectively.

To estimate sloshing-induced overflow, mass flow rate, $\dot{m}$ (kg/sec), is necessary to be first computed from FSI analysis. It indicates the mass of a substance (*e.g.*, fluid) that passes through an identified surface per unit time. $\dot{m}$ at the opening boundary is calculated as [2]:

$$\dot{m} = \rho \cdot A_i \cdot V_i \quad (1)$$

where ρ is the mass density of the fluid; A is the cross-sectional vector area/surface; V is the flow velocity of the mass elements; and i indicates the individual side walls in a rectangular tank (*i.e.*, east, west, north, south). Sloshing-induced overflow is then estimated by dividing the computed $\dot{m}$ in Eq. (1) into the fluid mass density. Accordingly, the total overflowed liquid volume, V_{tot} (m^3), measured in four-side walls is given by:

$$V_{tot}(t) = \int_0^t \frac{\dot{m}_E(t) + \dot{m}_W(t) + \dot{m}_N(t) + \dot{m}_S(t)}{\rho} \cdot dt \quad (2)$$

where $\dot{m}_E$, $\dot{m}_W$, $\dot{m}_N$, and $\dot{m}_S$ are the mass flow rate in each side wall.

In this study, a two-way FSI analysis is performed to estimate liquid overflow for all identified cases, by using common finite element (FE) software programs ANSYS and CFX. It is assumed that fluid motion is ideally irrotational, incompressible, and inviscid. It is noted that this approach was already validated in the authors' previous work [5].
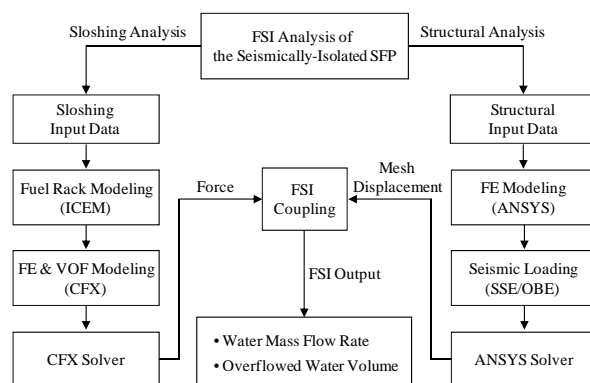

Fig. 1. Flowchart for FSI analysis.

2.2 Descriptions and FE Modeling of SFP with/without Fuel Racks

The seismically-isolated SFP, which is a pool-type rectangular reinforced concrete structure, is located in the auxiliary building. Its typical inner dimensions are 10.52 m (35 ft 6 in) in width and 12.80 m (42 ft) in length and height. Fluid filled in SFP is assumed to be water with its design free surface of 12.24 m (40 ft 2 in). The associated material properties are presented in Table I.

Table I: Material Properties

Parameter	SFP	Fluid (Water)
Young's modulus, E (GPa)	27.79	-
Poisson's ratio, v	0.17	-
Density, ρ (kg/m^3)	2,403	997
Free surface, h (m)	-	12.243

A 3-D FE modeling of SFP with fuel racks is developed. VOF method consisting of air and water regions is employed in liquid modeling, while the SFP structural modeling is developed using a solid element type (*i.e.*, solid185) is developed (see Fig. 2). Fuel storage racks designed to store spent fuel removed from nuclear reactors are assumed to be 4.775 m in height. It is also assumed that fuel racks consist of empty fuel cells in every 0.271 m. Rack-to-rack spacing is ignored. In this study, three different fuel-cell assemblies with the SFP only (i.e., any fuel racks are not included) are taken into account, as shown in Figs. 3 (a) to (d):
  (i) FR-0: not included fuel racks,
  (ii) FR-1: fuel cells inserted in Region A only,
  (iii) FR-2: fuel cells inserted in Regions A and B, and
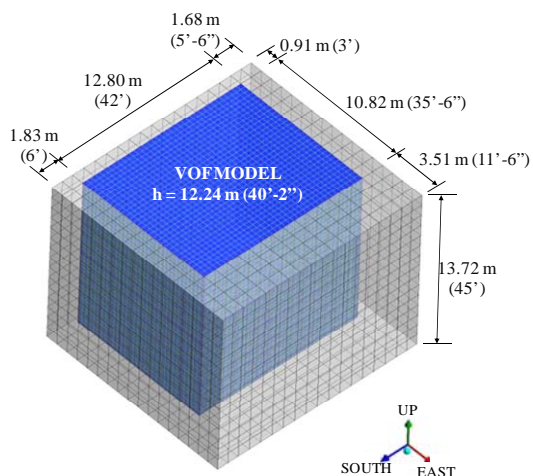 (iv) FR-3: fuel cells inserted in Regions A, B, and C
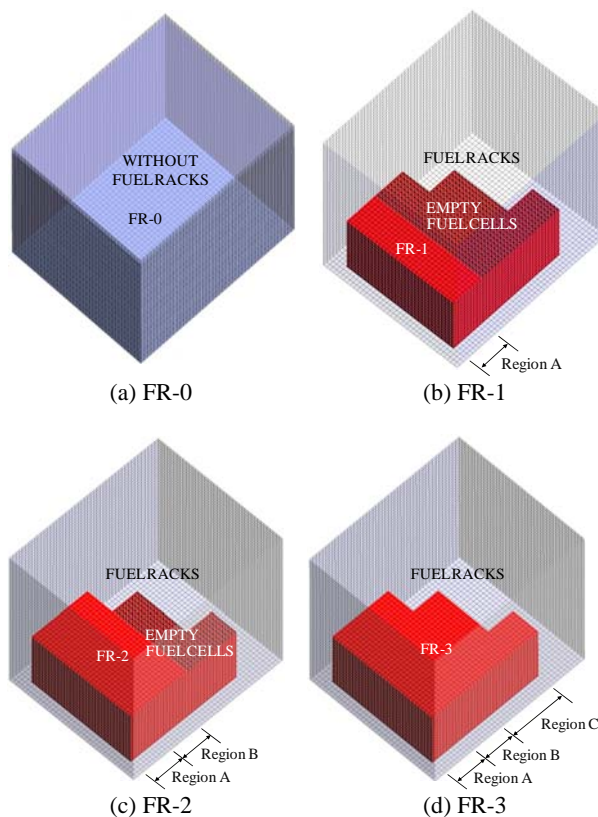

Fig. 2. Dimensions and FE modeling of SFP.

Fig. 3. Fuel racks modeling according to fuel-cell assemblies.

2.3 Seismic Loading

As a load effect, floor acceleration time-histories produced from the preliminary soil-structure interaction (SSI) analyses for a full beam-stick modeling of the seismically-isolated nuclear auxiliary building are imposed to the SFP base. These acceleration inputs were obtained by exciting three different PGAs (*i.e.*, 0.2g, 0.3g, and 0.5g) at bed rock level, as shown in Figs. 4 (a) to (c). The associated maximum floor accelerations are presented in Table II. For each PGA, three floor accelerations in east-west (EW), north-south (NS), and vertical (VT) directions are simultaneously imposed to the SFP base up to t = 20.48 sec. After that, additional zero excitations are lasted up to t = 40 sec to make sloshing behavior to be converged stably.

Table II: Maximum Instructure Accelerations for FSI Analysis

*PGA (g)	Maximum instructure acceleration (g)		
	EW	NS	VT
0.2	0.086	0.090	0.212
0.3	0.107	0.138	0.325
0.5	0.159	0.186	0.562

* PGA values imposed in vertical direction are obtained by scaling two-thirds the PGAs excited in horizontal direction.
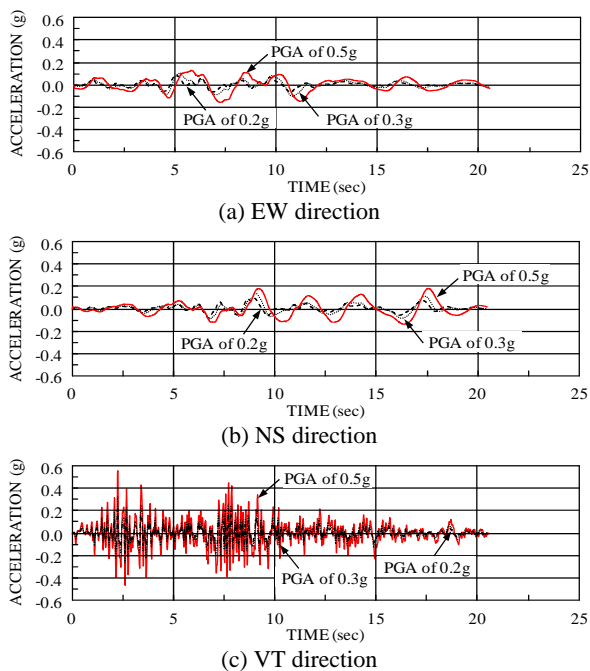
Fig. 4. Three sets of floor acceleration time-histories produced from different PGAs.

2.4 Effect of Fuel Racks on SFP Overflow Behavior for PGA of 0.5g

Effects of different fuel-cell assemblies on the SFP overflow is herein investigated. In a conservative way, a PGA of 0.5g is treated as a target value in design of the seismically-isolated SFP. As described previously, the floor accelerations produced from the target PGA are used as a seismic input in FSI analyses which are carried out to estimate the cumulative overflowed water volumes by using Eq. (2). At $t = 40$ sec, the cumulative overflowed water volumes are computed at the individual side walls and plotted with their summation (see Fig. 5). As shown in Fig. 5, the overflow difference is not significant for the identified cases (*i.e.*, FR-0, FR-1, FR-2, FR-3). By using V_{tot} measured by FR-0 as a reference value, the increase or decrease rate of each case is calculated. As presented in Table III, it is found that the maximum difference does not exceed about 4%. This small gap may be possible because sloshing frequency is not affected considerably in the existence of fuel racks. As a result, in liquid overflow assessment and prediction of the seismically-isolated SFP, fuel storage racks can be excluded to improve computation efficiency and produce more conservative outputs.

Figs. 6 and 7 show free surface profiles in FR-0 and FR-1, respectively. Similarly, the sloshing behavior in two cases FR-0 and FR-1 is not different. In both cases, the peak sloshing is occurred at the west-north corner wall at $t = 10.19$ sec. Fig. 8 shows the sloshing behavior of each case at $t = 40$ sec. Sloshing in FR-1, FR-2, and FR-3 is almost similar, whereas that in FR-0 is a little

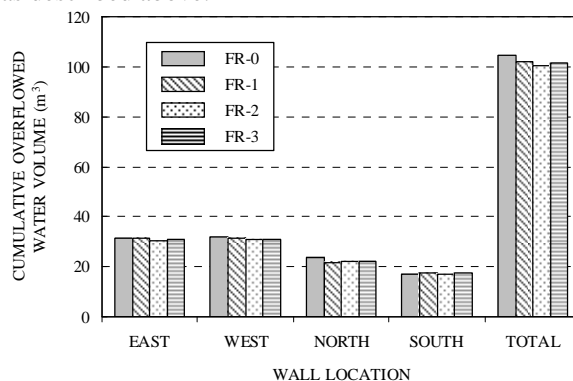fluctuated. However, the overflow difference is not big, as described above.

Fig. 5. Cumulative overflows according to different assemblies of fuel cells in SFP.

Table III: SFP Overflows Estimated in Each Case

Case	Total cumulative overflowed water volume at $t = 40$ sec (m³)	Rate (%)
*FR-0	104.34	RV
FR-1	102.15	(-) 2.10
FR-2	100.32	(-) 3.85
FR-3	101.69	(-) 2.54

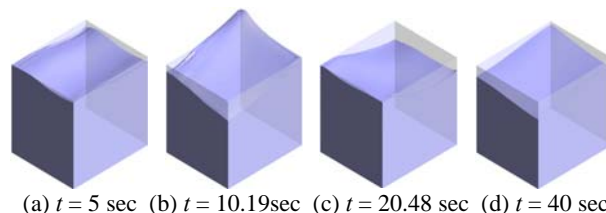* FR-0 is used as a reference value (RV) to compute the increase or decrease rate.

(a) $t = 5$ sec (b) $t = 10.19$sec (c) $t = 20.48$ sec (d) $t = 40$ sec

Fig. 6. Time-history sloshing behavior in FR-0.

(a) $t = 5$ sec (b) $t = 10.19$sec (c) $t = 20.48$ sec (d) $t = 40$ sec
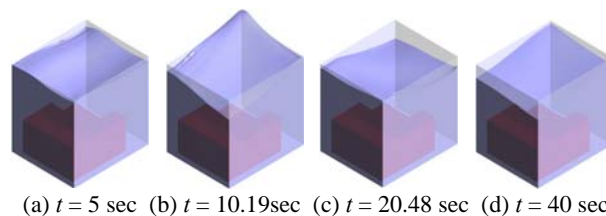
Fig. 7. Time-history sloshing behavior in FR-1.

(a) FR-0   (b) FR-1   (c) FR-2   (d) FR-3
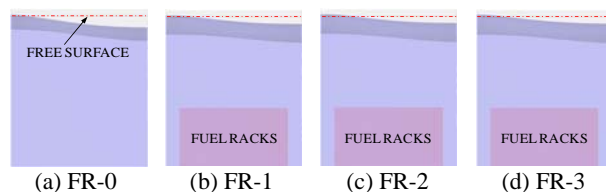
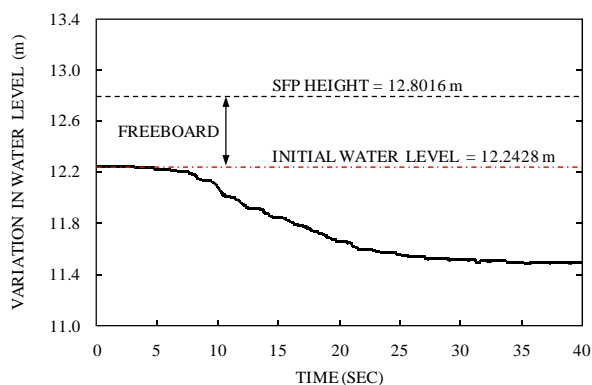Fig. 8. South view of sloshing behavior at $t = 40$ sec.

Fig. 9. Variation in water level under seismic excitations.

Fig. 9 shows the time-history profile of initial water level of the isolated SFP, under earthquake. Due to violent liquid sloshing from $t = 10$ sec to $t = 20$ sec, it is significantly reduced. For given design PGA of 0.5g, the total cumulative overflowed water volume exceeds about 75 cm at $t = 40$ sec.

2.5 SFP Overflow Assessment with Different PGAs

For a design free surface of 12.24 m, three different PGAs (*i.e.*, 0.2g, 0.3g, 0.5g) are excited at the isolated SFP base. As shown in Fig. 10, at $t = 40$ sec the minimum overflow of 33 m^3 is occurred in PGA of 0.2g, whereas the maximum overflow of 104 m^3 is observed in PGA of 0.5g (see also Table IV).
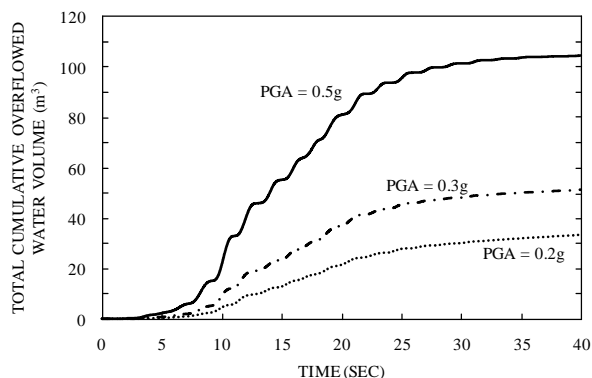

Fig. 10. SFP overflow profiles for different PGAs.

Table IV: SFP Overflows for Different PGAs

PGA	Cumulative overflows (m^3)		*Increase rate, *IR* (%)
	V_A, $t = 20.48$sec	V_B, $t = 40$sec	
0.2g	22.48	33.33	(+) 48.28
0.3g	37.91	51.07	(+) 34.71
0.5g	81.45	104.34	(+) 28.10

* IR (%) = 100·$(V_B - V_A)/V_A$.

In addition, Table IV presents the increase rate of overflows between $t = 20.48$ sec (end of seismic excitations) and $t = 40$ sec (additional zero excitations). It is observed that in relatively lower PGA of 0.2g, the overflow increase is significant. This may be acceptable because liquid sloshing in higher PGA can be more concentrated within seismic event (*i.e.*, $t = 20.48$ sec) such that additional overflow with zero accelerations is occurred to be relatively small.

3. Conclusions

An approach for the liquid overflow assessment of the seismically-isolated nuclear SFP with fuel storage racks based on FSI analysis was addressed. From the results of the identified cases, the following conclusions are drawn: (i) FSI technique can be effectively used to assess the seismically-isolated SFP overflow, (ii) In a conservative way, the isolated SFP without fuel racks can be used to assess its sloshing-induced overflow under earthquake since effect of fuel-cell assemblies on the SFP overflow is not significant, (iii) for given same conditions (*e.g.*, constant design free surface, same fuel-cell assembly) except seismic loading, the higher PGA is, the more liquid overflow increases, and (iv) to prevent unexpected overflow damages occurred in the seismically-isolated nuclear SFP, further research is needed for finding optimal design solutions associated with applicable minimum free surface, allowable drainage capacity, and so on.

REFERENCES

[1] M. Souli, D. J. Benson, Arbitrary Lagrangin-Eulerian and Fluid-Structure Interaction: Numerical Simulation, John Wiley & Sons, New Jersey, 2010.
[2] Ansys, Inc., Ansys CFX-Pre User's Guide Release 13.0, Canonsburg, PA, 2010.
[3] Ansys, Inc., Theory Reference for Ansys and Ansys Workbench Release 13.0, Canonsburg, PA, 2010.
[4] M. A. Goudarzi, S. R. Sabbagh-Yazdi, Investigation of Nonlinear Sloshing Effects in Seismically Excited Tanks, Soil Dynamics and Earthquake Engineering, Vol.43, pp.653-669, 2012.
[5] K. Kwon, H. T. Park, G. Y. Chung, S. Lee, Baffle Effects of the Seismically-Isolated Nuclear Tanks on Sloshing Reduction Based on FSI Analysis, Proceedings of 22nd SMiRT Conference, San Francisco, Paper ID 1004, 2013.